energy&fuels

pubs.acs.org/EF

Article

Microcosm Approach to Disentangle Bio-Oxidation and Photo-Oxidation Pathways in Macondo Well Oil: Molecular Characterization and Acute Toxicity Assessment

Published as part of Energy & Fuels special issue "Celebrating Women in Energy Research".

Huan Chen,* Amy M. McKenna, and Ryan P. Rodgers

Cite This: https://doi.org/10.1021/acs.energyfuels.4c03951

Read Online

ACCESS | Metrics & More | Article Recommendations | Supporting Information

ABSTRACT: When oil weathers in the environment, it undergoes oxidative transformations that increase its molecular complexity, influencing the fate, transport, and toxicity of the oil plume. The primary natural processes driving these transformations are photochemical- and microbial-oxidation. However, the relative contributions of each process to the postspill transformation of petroleum remain poorly understood. To address this, we utilized laboratory microcosms to evaluate the products of bio-oxidation and photo-oxidation independently. Electrospray ionization Fourier transform ion cyclotron resonance mass spectrometry (ESI FT-ICR MS) was employed to characterize the chemical evolution and degradation pathways of Macondo Crude oil (SRM 2779). Bio-oxidation microcosms were monitored for 30 days using live seawater filtered to capture the microbial population and resuspended in sterile artificial seawater. For comparison, a photo-oxidation microcosm and an early field sample collected after the *Deepwater Horizon* (DWH) spill were included. Results revealed distinct oxidation patterns: bio-oxidation releases a diverse range of oxyhydrocarbons into the water phase, while the oxygenated species in the field samples (oil-soluble) largely resemble photochemically oxidized products. Bio-oxidation does not significantly affect the composition of oil-soluble species but releases oxygenated transformation products into the water, containing 1−14 oxygen atoms. These low oxygen species (O_x) are initially oil-soluble but become water-soluble with increased oxygen incorporation. In contrast, photo-oxidation disproportionately contributes to the DOC pool, showing a 30-fold increase in DOC compared to bio-oxidation. Photo-oxidation nonselectively oxidizes petrogenic compounds, increasing the relative abundances of O_1 to O_{12} classes and generating abundant oil-soluble transformation products similar to those detected in field samples. Toxicity assessments using the Microtox bioassay suggest that the toxicity of photosolubilized carbon increases at early periods, while bacterial transformation products show a sustained decrease. These controlled microcosm experiments provide insights into the distinct oxidative processes affecting the fate and transport of oil components in the Gulf of Mexico.

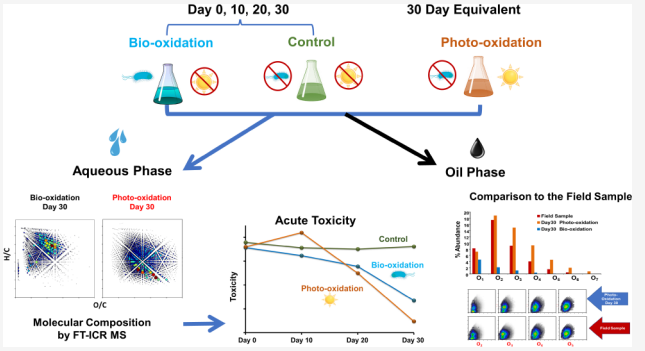

1. INTRODUCTION

The *Deepwater Horizon* (DWH) oil spill from April 20 to July 2, 2010 released approximately 5.0 million barrels of light sweet crude oil into the Gulf of Mexico (excluding collection efforts), posing significant risks to marine life, human health, and natural resources.[1] Saturated and aromatic compounds in the released oil transformed into polyfunctional oxygen-rich hydrocarbons with varying water solubility, bioavailability, and toxicity compared to the original oil.[2] These transformation products, being low in volatility, are challenging to detect using conventional gas chromatography (GC),[3] necessitating advanced analytical techniques such as Fourier transform ion cyclotron resonance mass spectrometry (FT-ICR MS) to elucidate petroleum weathering patterns at the molecular level.[4−6] Two major chemical weathering processes, photochemical oxidation (photo-oxidation) and microbial oxidation (bio-oxidation), play crucial roles in the transformation of petroleum hydrocarbons postspill. Photo-oxidation involves sunlight-driven reactions that introduce oxygen into petroleum hydrocarbons, forming a variety of oxygenated products. Recent studies, particularly in the context of the DWH spill, have highlighted the crucial role of photochemistry in the oxidation of floating oil. Ward et al. (2018) provided the first

Received: August 14, 2024
Revised: October 1, 2024
Accepted: October 9, 2024

definitive proof, through extensive field samples and environmentally relevant irradiation experiments, that photochemical reactions are the primary mechanism driving the oxidation of surface oil.[7] Sunlight-driven reactions produce oxygenated hydrocarbons, which are more water-soluble and alter the physical and chemical properties of the oil, making it more resistant to biodegradation.[8,9] In contrast, bio-oxidation involves bacterial metabolism that degrades hydrocarbons into simpler molecules, also introducing oxygen into the compounds, and can eventually remove the contaminant from the environment (mineralization).[10] However, biodegradation plays a relatively minor role in oil oxidation compared to photochemistry, as evidenced by limited changes in diagnostic biomarker ratios.[7] Additionally, indirect photolysis, driven by reactive oxygen species, has been identified as a dominant process for the degradation of oil residues in the marine environment.[11]

FT-ICR MS, with its high resolving power and mass accuracy, combined with selective ionization techniques, expands the analytical window for oil spill residues. This encompasses the entire upper carbon number range (C_{10} − C_{100}+) and heteroatom content (0−20+), which reveals the link between molecular composition and physical/chemical behavior.[12] Previous FT-ICR MS studies have revealed persistent polar oxygenated carboxylic acids in oil residues from coastal saltmarsh sediments impacted by the DWH spill, which persisted four years postspill.[13] These studies suggest that as oxygen content increases, compounds may become water-soluble and thus lost to water.[4] Such findings underscore the necessity of FT-ICR MS to address the molecular complexity of oil weathering products.[12]

Research has demonstrated significant molecular changes in oil residues revealed by FT-ICR MS due to photo-oxidation and bio-oxidation. For instance, Ruddy et al. observed increased complexity in Macondo well oil (MWO) residues from Pensacola Beach, which generated new species not present in the parent oil.[14] Harriman et al. examined the chemical composition of dissolved organic matter (DOM) leached from beach sand patties contaminated by the spill, revealing that photo-oxidation increased the rate of microbial degradation.[15] Photochemical degradation of crude oil is well-known, with decades of research focused on assessing oil degradation products derived from many oil spills.[16] Studies using solar simulators have demonstrated that sunlight-driven photo-oxidation significantly alters oil constituents, contributing to oil weathering.[17] Oil toxicity changes as oil degrades in the environment, and previous studies suggest that newly formed oxygenated hydrocarbons from photo-oxidation are more toxic than the precursor compounds.[6,18] Solar radiation absorbed by polyaromatic hydrocarbons (PAHs), known toxins, produces free radicals that react with oxygen to produce reactive oxygen species that can damage DNA and other cellular macromolecules.[19] Despite extensive research, the relative contributions of photo-oxidation and bio-oxidation to the overall transformation of petroleum hydrocarbons postspill remain unclear. Compositional trends observed in field samples require validation through controlled laboratory studies to disentangle potential biotic and abiotic modifications that can occur in parallel.

To address this knowledge gap, we conducted controlled laboratory microcosm experiments to evaluate the biological degradation pathways of crude oil. These microcosms exclusively focused on biological degradation, isolating the effects of bio-oxidation (Bio-Ox) from photo-oxidation (Photo-Ox). We quantified the bulk dissolved organic carbon (DOC) to determine the amount of oil entering the water and used FT-ICR MS to track the molecular transformation of MWO in both the organic (oil-soluble) and aqueous (water-soluble) phases. Additionally, we employed the Microtox[6,20] bioassay to temporally track changes in the toxicity of petroleum transformation products after microbial degradation. This study aims to characterize biotic modifications of crude oil at the molecular level, to provide insights into the compounds released into water from oil contaminants and to compare the composition of the source oil to Bio-ox products to elucidate how bacterial communities modify these compounds. Understanding these processes is crucial for assessing the environmental impact of oil spills and developing effective remediation strategies.

2. EXPERIMENTAL SECTION

2.1. Biodegradation and Photo-Oxidation Microcosm Setup. To investigate the biodegradation process, Bio-Ox microcosms were established by adding 1540 μL of Macondo crude oil SRM 2779 (Standard Reference Material, National Institute of Standards and Technology, Gaithersburg, MD) into 200 mL of autoclave-sterilized 70% artificial seawater (ASW) (Instant Ocean Aquarium Systems Inc., Mentor, OH, USA). This volume of oil formed a 120 μm oil film. All flasks (precombusted in a muffle furnace (450 °C for 4 h)), were wrapped in foil and shaken overnight. The oil-to-water ratio was kept consistent with previous photo-oxidation experiments (published separately)[4] to facilitate comparisons between the two processes (photo- and bio-oxidation). Live seawater was collected from the Gulf of Mexico (Latitude: 29° 54′ 49.6″ N; Longitude: 84° 30′ 41.7″ W; Temperature: 23.1 °C; Salinity: 30.8 ppt; pH: 8.1; Dissolved oxygen: 5.21 mg/L). The water samples were stored on ice and transported to the National High Magnetic Field Laboratory (Tallahassee, Florida) within 3 h of collection. The seawater was filtered through 0.8 μm membrane filters to remove debris and large organisms. Subsequent filtration through 0.2 μm membrane filters captured the microbial population, which was then resuspended directly in the same amount of sterile ASW.

Control microcosms consisted of sterile ASW and oil, without bacteria. Both test and control microcosms were wrapped in foil to prevent photo-oxidation and incubated on a Thermo Scientific MaxQ 4000 orbital shaker, shaken at 110 rpm and 23 °C (Figure S1, left). Each microcosm was monitored at ten-day intervals for 30 days. Microcosms were prepared in triplicate for each treatment to ensure reproducibility. Each microcosm consisted of same amount of ASW and oil and used the same incubation and mixing procedures. A 30-day equivalent photo-oxidation microcosm was also established for comparison (irradiated for a maximum of 180 h under a solar simulator) (Figure S1, right). The photoirradiation was set at 756 W/m^2, roughly equivalent to 4 days of natural sunlight per 24 h of photoirradiation in the solar simulator.[4,21] Samples were collected every 6 h for early time points and every 24 h for later time points.[4] The final point was collected after 180 h of irradiation, equivalent to 30 days of natural sunlight. For Bio-Ox, we limited our microcosm length to t = 30 days to avoid disruption of the microbial population (bottle effect).[22] We used ASW because it sustains microbial populations for microcosm experiments[23] and provides a clean mass spectral background, as it is free of dissolved organic matter present in natural seawater, which could otherwise interfere with the experimental results. An early slick sample (Juniper), collected about 90 days after the start of DWH spill, was used as a field sample for comparison. All solvents were HPLC grade (Sigma-Aldrich Chemical Co., St. Louis, MO).

2.2. Extraction of Water-Soluble Organics (WSO) and Oil from Microcosms. At each time point (0, 10, 20, and 30 days, Bio-Ox and 0, 6, 12, 18, 24, 48, 72, 96, 120, and 180 h irradiation, Photo-Ox), the water layer of the microcosms was transferred to a sterile

https://doi.org/10.1021/acs.energyfuels.4c03951
Energy Fuels XXXX, XXX, XXX−XXX

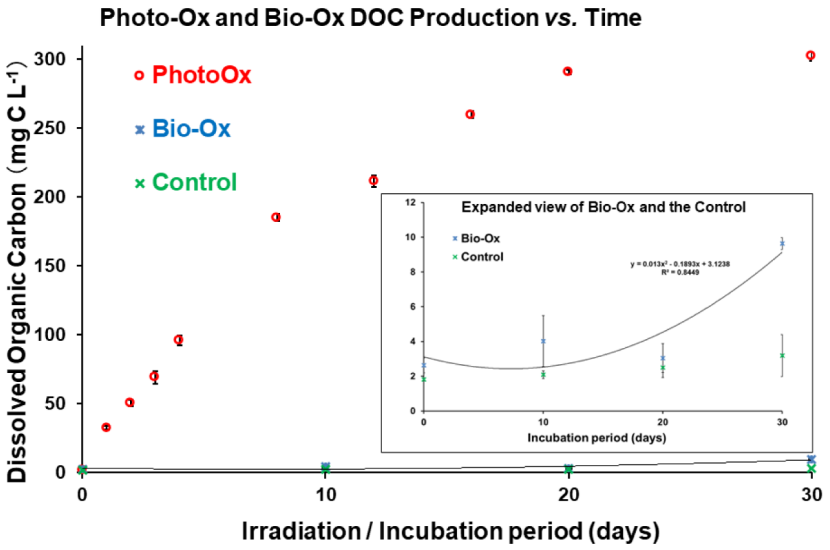

Figure 1. Dissolved organic carbon (DOC) concentrations in Bio-Ox and control (sterile) microcosms over a 30-day incubation period. The Bio-Ox microcosm shows a nonlinear increase in DOC, particularly after 20 days, suggesting enhanced microbial activity. In contrast, the control microcosm exhibits only a minimal increase in DOC, indicating limited transformation in the absence of bacterial modification. The polynomial fit (R^2 = 0.8449) illustrates the trend in DOC production over time. Error bars represent standard deviations of triplicate measurements.

container using a sterile glass pipet. The water fractions were then filtered through 0.2 μm membrane filters to remove the microbial population. Twenty milliliters of each sample were acidified to pH 2 with HCl, and the water-soluble organics were extracted using a solid-phase extraction method.[24] Briefly, acidified samples were loaded onto a Bond Elut PPL (Agilent Technologies) stationary phase cartridge, desalted with pH 2 water, and eluted with methanol to a final concentration of 100 μg/mL prior to FT-ICR MS analysis.

The remaining oil layer in the microcosms was dissolved in toluene, transferred to a clean vial, and dried under nitrogen. The dried oil was topped with argon gas and stored at 4 °C for FT-ICR mass spectral analysis. A 4 mL aliquot of each water sample was stored at 4 °C for toxicity analysis. The experimental flowchart is provided (Figure S2).

2.3. Dissolved Organic Carbon Measurement. Dissolved organic carbon (DOC) concentrations were determined using a Shimadzu TOC-V WS analyzer (Shimadzu Corp., Japan).[4] Each sample was diluted with deionized water in a ratio of 20 mL sample to 20 mL water. Samples were then acidified to a pH of 2 with H_3PO_4, with a 3% acid injection per sample. The coefficient of variance (precision) was <2% for replicate determinations.

2.4. Fourier Transform Ion Cyclotron Resonance Mass Spectrometry. Prior to FT-ICR mass spectral analysis, the oil-soluble species were diluted in toluene to make a stock solution (1 mg/mL), which was further diluted to a final concentration of 250 μg/mL with equal parts (vol) methanol, spiked with 0.25% tetramethylammonium hydroxide (TMAH, 25% by weight in methanol) to ensure efficient deprotonation for negative-ion ESI. Water-soluble organic species were analyzed by negative-ion ESI without a modifier. The FT-ICR mass spectrometer is custom-built with a 9.4 T superconducting magnet.[25] Detailed ionization source conditions and FT-ICR MS conditions can be found in the Supporting Information.

2.5. APS Fractionation. Isolation and fractionation of crude oil compounds on aminopropyl silica (APS) were conducted to identify compounds with acidic functional groups.[26] Briefly, carboxylic acid-containing compounds interact via strong hydrogen bonding with APS and are eluted based on hydrophobicity. Nonacidic compounds elute with dichloromethane (DCM) in fraction 1; moderately acidic species elute in fraction 2 with DCM-methanol; and carboxylic acids elute in fraction 3 with the addition of formic acid. APS separation was used to quantify the oil-soluble acid-containing compounds resulting from Bio-Ox.

2.6. Toxicity Assessment. The Microtox toxicity analysis was employed to monitor the toxicity of water-soluble petroleum transformation products collected at various intervals, following the same method as previously published.[4] Water extracts from both the experimental and control microcosms were carbon-normalized to a concentration of 1.7 μg/mL based on dissolved organic carbon (DOC) prior to Microtox testing. The toxicity of each water fraction over all time intervals was determined by measuring the reduction in bioluminescence of the bacterium *Aliivibrio fischeri*. The Microtox 81.9% screening test protocol was conducted using the Microtox model 500 analyzer (Modern Water, New Castle, DE, USA).[27]

3. RESULTS AND DISCUSSION

3.1. Bio-Ox Increases DOC Levels but Remains Lower Compared to Photo-Ox. Our experiments revealed distinct differences in the production of dissolved organic carbon (DOC) between the Bio-Ox and Photo-Ox microcosms. As shown in Figure 1, DOC levels remained relatively unchanged during the first 20 days of the Bio-Ox microcosm. However, by day 30, DOC levels in the Bio-Ox microcosm reached 9.6 ± 0.3 mg C/L, which is approximately three times higher than the control microcosm, where DOC levels were 3.2 ± 1.2 mg C/L. The fitted curve (R^2 = 0.8449) highlights the nonlinear nature of DOC production in the Bio-Ox microcosm, which highlights an initial lag phase followed by a clear acceleration in the later stages of the incubation period. This delayed increase in DOC suggests that microbial activity becomes more significant after the initial 20-day period, possibly due to the adaptation and proliferation periods of the microbial community.

In contrast, the Photo-Ox microcosm showed a rapid and substantial increase in DOC, with levels reaching 302.3 ± 3.0 mg C/L after the equivalent of 30 days of solar irradiation (180 h). This represents a 30-fold increase compared to the DOC levels in the Bio-Ox microcosm and highlights the effectiveness of photochemical processes in breaking down oil components. These results are consistent with previous studies, where similar DOC concentrations were observed in photo-oxidized oil samples, such as 189.9 mg C/L with BP surrogate oil[6] and 290.0 mg C/L with NST SRM 2779 after 120 h of solar

https://doi.org/10.1021/acs.energyfuels.4c03951
Energy Fuels XXXX, XXX, XXX−XXX

exposure.[4] The large contrast between Bio-Ox and Photo-Ox in DOC production highlights the different pathways and efficiencies of these oxidation processes. While Bio-Ox primarily acts on more aliphatic (biolabile) components over time, leading to a steady but moderate increase in DOC, Photo-Ox rapidly, directly oxidizes a broad range of aromatic (chromophore-containing) species and indirectly oxidizes nearly all oil constituents, which results in a significant and immediate increase in water-soluble organic carbon.

3.2. Bio-Ox Generates Highly Oxygenated Transformation Products in the Water Phase. The molecular characterization of the water-soluble organic species produced by Bio-Ox via FT-ICR MS revealed a significant progression in both oxygen content and molecular complexity over the 30-day incubation period. This transformation results in an increasing number of mass spectral peaks and the evolution of the oxygen class distributions. As shown in Figure S3, the expanded segments of the mass spectra from m/z 395−400 demonstrate a clear trend of increasing oxygenation and spectral complexity from day 10 to day 30 in the Bio-Ox microcosms. On day 10, the Bio-Ox microcosm produced 294 mass spectral peaks, including species containing up to 8 oxygen atoms per molecule. By day 20, this number increased to 340 peaks, with higher oxygenated species, such as O_8 and O_9, becoming more prominent. By day 30, the complexity further increased to 503 peaks, with species containing up to 10 oxygen atoms.

Figure 2 further supports this progression and reveals the distribution of oxygen classes (O_x) in the water-soluble organics from the Bio-Ox microcosms at 10, 20, and 30 days, as well as from a 30-day Photo-Ox microcosm for comparison. Early in the Bio-Ox incubation (day 10), the dominant oxygen classes were O_2 and O_3, corresponding to simpler oxygenated compounds such as carboxylic acids and alcohols. As the incubation progressed, the relative abundance of higher oxygen classes, particularly O_6 to O_8, increased significantly, indicating the formation of more complex polyfunctional species. By day 30, the Bio-Ox microcosm had shifted toward even higher oxygen content, with O_7−O_{10} classes becoming more prominent. This progression suggests that microbial oxidation not only introduces more oxygen into the original oil molecules but also facilitates the formation of increasingly complex structures over time, likely responsible for the observed decrease in toxicity in the water-soluble fraction (discussed in section 3.4). In comparison, the Photo-Ox microcosm displayed a broader and more even distribution of oxygen classes ranging from O_1 to O_{12} (Figure 2). This difference highlights the more rapid and nonselective nature of photochemical oxidation,[25] which increases the oxygen content across a wide array of molecular species, which yields a unique profile of water-soluble organics than that produced by microbial activity. The use of FT-ICR MS, with its exceptional mass resolution (>800,000 at m/z 400), was instrumental in capturing the molecular-level changes in the water-soluble organic fractions. This ultrahigh-resolution capability enabled us to distinguish thousands of oxygenated compounds, highlighting the unique advantages of FT-ICR MS in detecting complex transformations during oil degradation that would otherwise remain unresolved by conventional techniques, such as GC-FID.

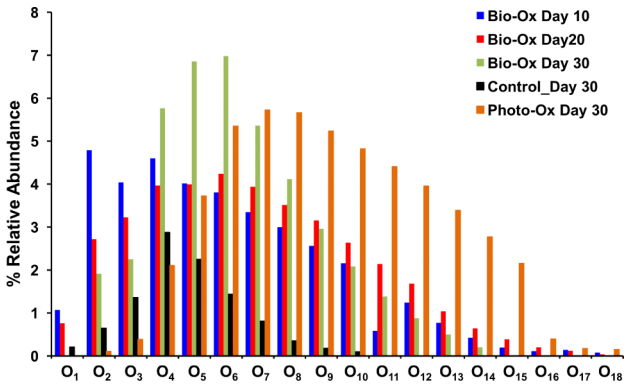

Figure 2. Oxygen class distribution derived from ESI (−) FT-ICR MS analysis of water-soluble organics isolated from 10, 20, and 30-day Bio-Ox microcosms, Bio-Ox control, and a 30-day Photo-Ox microcosm.

3.3. Bio-Ox and Photo-Ox Yield Distinctive Oxidation Signatures in Water. The FT-ICR MS analysis revealed that Bio-Ox and Photo-Ox processes generate distinctive oxidation signatures in the water-soluble fractions of oil, evident through differences in molecular characteristics and distributions of hydrogen-to-carbon (H/C) and oxygen-to-carbon (O/C) ratios. Figure 3 presents a series of van Krevelen diagrams for water-soluble species generated in the Bio-Ox microcosms at 10, 20, and 30 days, alongside the 30-day Photo-Ox microcosm. Over time, the Bio-Ox samples exhibit a progressive shift toward higher O/C ratios while maintaining a relatively narrow H/C range, primarily between 1.0 and 2.0. This indicates that microbial oxidation processes are selective, and predominantly target aliphatic oil components that favor the production of oxygenated species with consistent structural characteristics (high H/C species), which is well documented in the petroleum biodegradation literature. In contrast, the 30-day Photo-Ox microcosm shows a broader distribution in both O/C to H/C ratios, spanning a wider range of molecular structures. The more extensive spread in the van Krevelen diagram reflects the nonselective nature of photochemical oxidation,[25] which affects a broader variety of petrogenic compounds. This broader range of oxidation products suggests that photo-oxidation can generate a more diverse array of water-soluble organics compared to the more selective bio-oxidation process.

Figure 4 provides a deeper insight into the specific O_2 class species detected in the water-soluble organics (WSO) from the 30-day Bio-Ox and 30-day Photo-Ox microcosms. In the Bio-Ox microcosm, the O_2 species contain higher double bond equivalence (DBE) values, indicative of more complex and aromatic structures. Notably, specific compounds such as those with m/z 185.06082 (DBE 8), m/z 199.07646 (DBE 8), and m/z 177.09210 (DBE 5) are potential biomarkers of bio-oxidation. These species, which are accompanied by lower DBE, steric (cycloalkane) and fatty (alkane) acids, are indicative of the selective degradation pathways favored by microbial communities. In the Photo-Ox microcosm, the O_2 species show a different distribution, with notable signals at m/z 189.09213 (DBE 9), m/z 217.12341 (DBE 6), and m/z 191.10775 (DBE 5, also observed in Bio-Ox). The presence of these species indicates that photochemical oxidation affects a broader spectrum of molecular structures, including both aromatic and aliphatic hydrocarbons. This diversity suggests the nonselective nature of photochemical processes, which can produce a wide array of oxygenated species, some of which overlap with those generated by microbial oxidation.

https://doi.org/10.1021/acs.energyfuels.4c03951
Energy Fuels XXXX, XXX, XXX−XXX

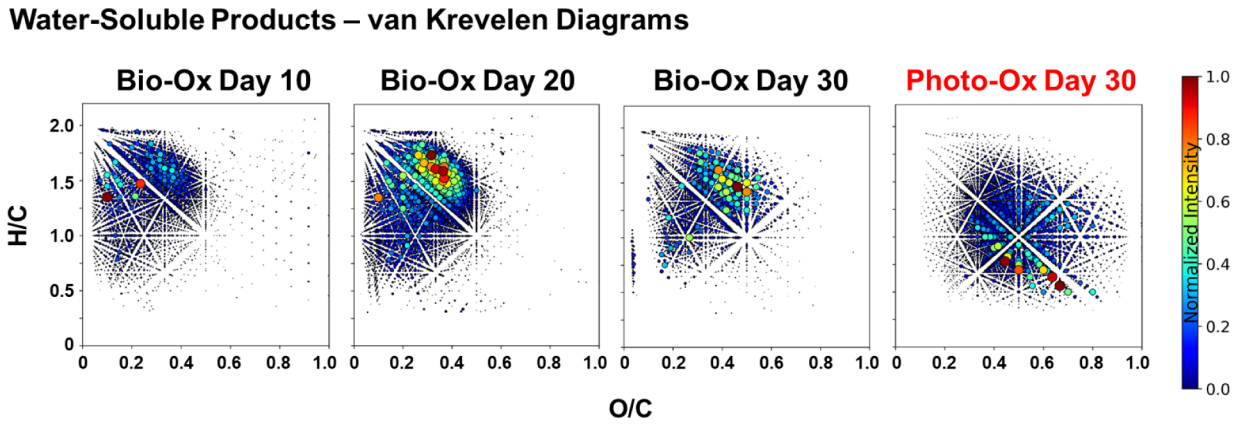

Figure 3. van Krevelen diagrams of water-soluble species generated in Bio-Ox microcosms after 10, 20, and 30 days of incubation, compared to a 30-day Photo-Ox microcosm.

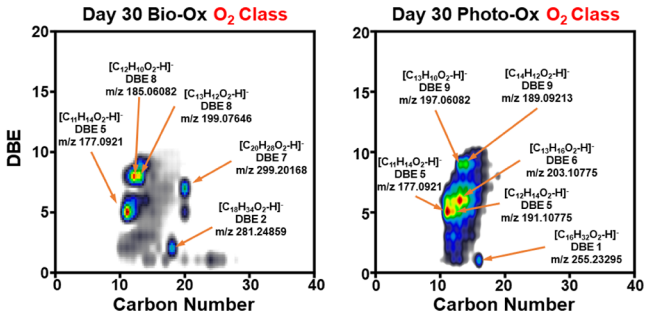

Figure 4. Double bond equivalence (DBE) versus carbon number plots for O_2 class species in the water-soluble organics from 30-day Bio-Ox and 30-day Photo-Ox microcosms.

Summation of all Ox species (O_1–O_{max}), yields the global trends highlighted in the van Krevelen diagrams (Figure 3).

The contrasting profiles of O_2 species in Bio-Ox and Photo-Ox microcosms, combined with the global summation of all oxygen-containing species observed, highlight the complex and complementary roles these processes play in the environmental transformation of oil. While Bio-Ox leads to the formation of more complex, aromatic-rich oxygenated species in low oxygen-content species, Photo-Ox generates a broader range of oxidation products, impacting a wider variety of molecular structures. However, as oxygen-content increases, the DBE range of Bio-Ox products increases much more slowly than for Photo-Ox. Ultimately, this yields the trends highlighted for all Ox species (Figure 3). The specific O_2 species identified in both microcosms, particularly those unique to each oxidation process, could serve as molecular markers used to distinguish between microbial and photochemical degradation pathways in environmental monitoring and oil spill remediation efforts. Future studies, including tandem MS (MS/MS) analysis, will be crucial to further characterize the structures of these potential biomarkers and to elucidate the mechanisms behind their formation. The ability to distinguish between Bio-Ox and Photo-Ox signatures using specific molecular markers could have significant implications for understanding the environmental fate of oil spills and for developing targeted remediation strategies.

While our extraction and analytical methods were optimized to recover and analyze neutral and acidic compounds, it is important to acknowledge that basic weathering products, such as nitrogen-containing compounds, may have been underrepresented. These compounds, which can form during both photochemical and microbial degradation processes, are typically less abundant but still contribute to the overall transformation of oil residues. Future studies should consider employing additional extraction methods that target basic functionalities to provide a more complete understanding of oil degradation. Despite this limitation, our results remain robust in demonstrating that neutral and acidic compounds are the primary products of photochemical oxidation, and the dominance of these processes in oil weathering remains clear.

3.4. Acute Toxicity Trends in Bio-Ox and Photo-Ox Water-Soluble Species. The toxicity of WSO derived from the Bio-Ox and Photo-Ox microcosms was evaluated using the Microtox bioassay, with a focus on acute toxicity per unit carbon as measured by the inhibition of bioluminescence from *Aliivibrio fischeri*. Microtox has been widely used for its rapid and high-throughput screening capability, providing insight into the potential ecological impacts of complex mixtures such as oil weathering products.[28] Figure 5 shows the trends in acute toxicity over the 30-day incubation period for Bio-Ox, Photo-Ox, and control microcosms. The results indicate that the Bio-Ox microcosm (Figure 5) exhibits a significant decrease in toxicity over time. The quadratic fit applied to

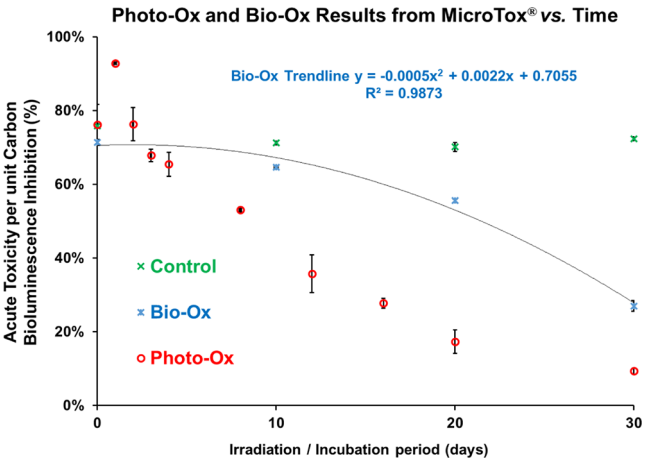

Figure 5. Acute toxicity per unit carbon, measured as bioluminescence inhibition (%), of water-soluble organics (WSO) for the Bio-Ox, Photo-Ox, and control microcosm over a 30-day incubation/irradiation period. Error bars represent the standard deviation of triplicate measurements.

https://doi.org/10.1021/acs.energyfuels.4c03951
Energy Fuels XXXX, XXX, XXX−XXX

the Bio-Ox data (R^2 = 0.9873) in Figure 5 depicts the gradual decline in toxicity over time, further highlight the detoxifying potential of microbial oxidation. At the beginning of the incubation period, the acute toxicity of the Bio-Ox WSO was relatively high, with over 70% bioluminescence inhibition, indicating notable toxicity. However, by day 30, the toxicity had decreased to less than 20% bioluminescence inhibition. This reduction suggests that microbial activity not only transforms oil-derived compounds but also reduces their toxicity, potentially through processes that lead to the formation of less harmful, more oxygenated species as discussed in Sections 3.2 and 3.3.

In contrast, the Photo-Ox microcosm displayed a different trend. Photo-oxidation initially increased the toxicity of oil-derived WSOs, with toxicity peaking within the first 6 h of irradiation (at >90%) and then gradually decreased over time.[4] In our study, the toxicity of the Photo-Ox microcosm was measured at 9.4 ± 0.1% at day 30, even lower than the toxicity in day 30 Bio-Ox microcosm. The control microcosm, which lacked bacterial and photochemical modification, showed minimal changes in toxicity over time. This stability in toxicity levels suggests that without active oxidation processes, the inherent toxicity of the oil-derived WSO remains largely unchanged. The contrasting results between Bio-Ox and Photo-Ox highlight the differing environmental impacts these processes may have in future spills. These findings suggest the importance of considering both biological and photochemical oxidation pathways in the environmental management of oil spills. While both processes contribute to the degradation of oil, their effects on the toxicity of the resulting transformation products are markedly different, with implications for the long-term health of affected ecosystems. However, it is important to acknowledge the limitations of the Microtox assay. While it offers valuable information about acute toxicity, particularly in the water-soluble fraction, it does not capture the full spectrum of toxicological effects that may occur over longer exposure periods or in different organisms.

3.5. Bio-Ox vs Photo-Ox: Contribution to Oil-Soluble Compounds. Previous studies have established that photochemical processes are the dominant degradation mechanism for DWH oil slicks, with bacterial modification of oil compounds being relatively minimal.[29] The current microcosm studies further support this observation, demonstrating that biodegradation results in only minor modifications to the acidic species in the oil layer, whereas photo-oxidation leads to significant chemical changes. Figure S4 shows that after 30 days of microbial degradation, the oil phase in the Bio-Ox microcosm exhibits minimal change compared to the control. The heteroatom class distribution (Figure S4a) shows that the relative abundances of various classes, including O_1 to O_7, remain consistent with those in the control. The DBE versus carbon number plots (Figure S4b) provide further support, showing that the composition of the Bio-Ox oil phase closely mirrors that of the control, with only slight variations that do not significantly alter the overall chemical profile. This indicates that Bio-Ox has a negligible impact on the oil-soluble fraction of the crude oil.

In contrast, the Photo-Ox process has a much more significant effect on the oil-soluble fraction. Photoirradiation nonselectively oxidizes petrogenic compounds, leading to a substantial increase in oxygenated hydrocarbons, such as hydroxyl, ketone, and carboxylic acid functionalities. These changes are similar to those observed in field samples collected after the DWH spill. Figure S5 shows the O_x class distribution after 30 days of solar exposure in the Photo-Ox microcosm, compared to an early slick sample field sample (Juniper) collected after the spill. The high degree of similarity between the Photo-Ox and field samples highlights the dominant role of photochemical processes in the environmental weathering of surface oil. Moreover, Figure 6 provides a direct comparison of

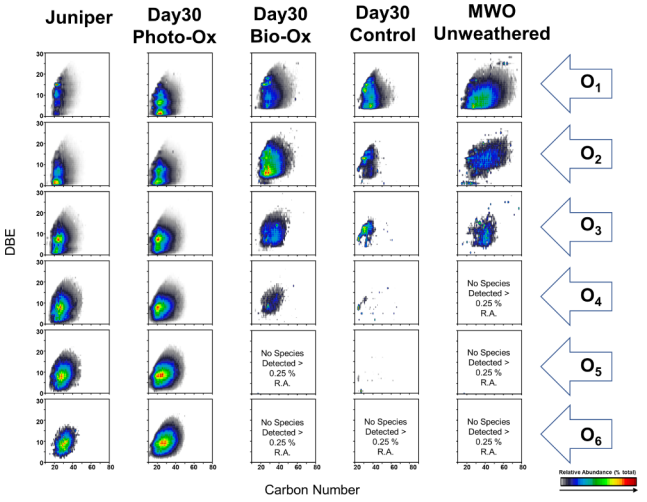

Figure 6. Double bond equivalence (DBE) versus carbon number plots for oxygenated species (O_1–O_6 classes) in oil-soluble compounds from the Juniper field sample, Day 30 Photo-Ox, Day 30 Bio-Ox, Day 30 Control, and MWO Unweathered oil.

DBE versus carbon number plots for Bio-Ox, Photo-Ox, and the Juniper field sample. The species generated by Photo-Ox align closely with those detected in the field sample, particularly within the O_1 to O_6 classes. This strong correspondence confirms that the photo-oxidation process produces oil-soluble compounds that are chemically similar to those found in the environment, further emphasizing the limited role of Bio-Ox in altering the oil phase.

The data in Table S1 reinforce this conclusion. Quantitation of acid-containing compounds through APS fractionation shows that the increase in acidity observed in DWH-contaminated sediment in Louisiana Saltmarshes over 4 year period[13] is not observed in the Bio-Ox microcosm. After 30 days, the acid levels in the Bio-Ox microcosm remain similar to those in the control (~1 wt %), compared to >9 wt % in photo-impacted sediments, suggesting that bacterial processes do not significantly contribute to the production of oil-soluble acids. Overall, these findings demonstrate that Bio-Ox has a minimal impact on the oil-soluble fraction of the crude oil, while Photo-Ox significantly alters the chemical composition, producing species that closely resemble those observed in environmental field samples. This highlights the dominant role of photochemical processes in the environmental weathering of DWH Oil Spill. While our study primarily used FT-ICR MS to provide a detailed molecular characterization of the water-soluble and oil-soluble organics, we acknowledge the importance of GC-FID for assessing nonpolar hydrocarbon fractions, including *n*-alkanes. GC-FID analysis could help document the compositional changes in the oil residues, particularly in relation to evaporation losses and microbial degradation, through monitoring key ratios such as n-C_{17} to pristane and n-C_{18} to phytane. Studies employee this technique

https://doi.org/10.1021/acs.energyfuels.4c03951
Energy Fuels XXXX, XXX, XXX−XXX

have shown that minimal changes in these diagnostic ratios suggest limited microbial oxidation, consistent with our conclusions.[7,30]

4. CONCLUSIONS

Our study presents a detailed examination of the distinct molecular signatures and environmental impacts resulting from bio-oxidation and photo-oxidation of Macondo well oil. Through controlled microcosm experiments, we have disentangled the contributions of these two oxidative processes and provided new insights into the fate of oil components in marine environments. Our findings demonstrate that Bio-Ox primarily generates water-soluble transformation products, characterized by a gradual increase in oxygenation and molecular complexity over time. These microbial processes preferentially produce highly oxygenated, low double bond equivalent (DBE) species, which, importantly, do not significantly alter the oil-soluble fraction of the crude oil. The reduction in toxicity observed in Bio-Ox microcosms highlights the detoxifying potential of microbial activity over extended periods. In contrast, Photo-Ox significantly alters the chemical composition of both water-soluble and oil-soluble fractions. Photo-oxidation rapidly produces a broad range of oxygenated hydrocarbons, including species that closely resemble those found in field samples from the DWH Spill. The nonselective nature of Photo-Ox leads to the formation of a diverse array of transformation products, including many that contribute to increased acute toxicity during the early time period of solar exposure. Our data demonstrates the dominant role of photochemical processes in the environmental weathering of oil spills, with Photo-Ox contributing more significantly to the transformation of oil-soluble species than Bio-Ox. While our study is focused on the DWH spill, it is important to note that the rates of photodegradation and bio-oxidation may vary depending on the source of the spilled oil and environmental factors such as solar intensity and temperature. However, the underlying degradation mechanisms remain similar across different spill scenarios, making these findings broadly applicable to other oil spills. These findings have important implications for understanding the long-term environmental impact of oil spills and for developing more effective strategies for monitoring and remediation. Future research should focus on the detailed structural characterization of the oxidation products formed by both processes, particularly those that overlap in DBE and carbon number ranges, to further elucidate their environmental behavior and toxicity.

ASSOCIATED CONTENT

Supporting Information

The Supporting Information is available free of charge at https://pubs.acs.org/doi/10.1021/acs.energyfuels.4c03951.

ESI source and 9.4 FT-ICR; mass calibration and data analysis; separation of naphthenic acids; bio-oxidation and photo-oxidation microcosm setup; experimental design of microcosm experiment; expanded segment of the mass spectra; negative-ion ESI; oxygen class distribution of oil-soluble compounds; percent recovery of each fraction and total percent recovery for APS acid extractions (PDF)

AUTHOR INFORMATION

Corresponding Author

Huan Chen − *National High Magnetic Field Laboratory, Florida State University, Tallahassee, Florida 32310-4005, United States;* orcid.org/0000-0002-6032-6569; Email: huan.chen@magnet.fsu.edu

Authors

Amy M. McKenna − *National High Magnetic Field Laboratory, Florida State University, Tallahassee, Florida 32310-4005, United States; Department of Soil and Crop Sciences, Colorado State University, Fort Collins, Colorado 80523-1170, United States;* orcid.org/0000-0001-7213-521X

Ryan P. Rodgers − *National High Magnetic Field Laboratory, Florida State University, Tallahassee, Florida 32310-4005, United States;* orcid.org/0000-0003-1302-2850

Complete contact information is available at: https://pubs.acs.org/10.1021/acs.energyfuels.4c03951

Notes

The authors declare no competing financial interest.

ACKNOWLEDGMENTS

This work was supported by a grant from the Gulf of Mexico Research Initiative, the National Science Foundation Division of Chemistry, Natural Sciences, and Division of Materials Research through DMR-1655779 and DMR-2128556, and the State of Florida. Data are publicly available through the Gulf of Mexico Research Initiative Information & Data Cooperative (GRIIDC) at DOI: 10.7266/n7-3d8b-0860. The authors thank Dr. Collin P Ward for providing the field sample. The authors also thank Sarajeen Saima Hoque for the DOC measurement.

REFERENCES

(1) McNutt, M. K.; Camilli, R.; Crone, T. J.; Guthrie, G. D.; Hsieh, P. A.; Ryerson, T. B.; Savas, O.; Shaffer, F. Review of flow rate estimates of the *Deepwater Horizon* oil spill. *P. Natl. Acad. Sci. U. S. A.* **2012**, *109* (50), 20260−20267.

(2) Aeppli, C.; Carmichael, C. A.; Nelson, R. K.; Lemkau, K. L.; Graham, W. M.; Redmond, M. C.; Valentine, D. L.; Reddy, C. M. Oil weathering after the *Deepwater Horizon* disaster led to the formation of oxygenated residues. *Environ. Sci. Technol.* **2012**, *46* (16), 8799−8807.

(3) Gough, M. A.; Rowland, S. J. Characterization of unresolved complex mixtures of hydrocarbons in petroleum. *Nature* **1990**, *344*, 648−650.

(4) Chen, H.; McKenna, A. M.; Niles, S. F.; Frye, J. W.; Glattke, T. J.; Rodgers, R. P. Time-dependent molecular progression and acute toxicity of oil-soluble, interfacially-active, and water-soluble species reveals their rapid formation in the photodegradation of Macondo Well Oil. *Sci. Total Environ.* **2022**, *813*, 151884.

(5) Wise, S. A.; Rodgers, R. P.; Reddy, C. M.; Nelson, R. K.; Kujawinski, E. B.; Wade, T. L.; Campiglia, A. D.; Liu, Z. Advances in chemical analysis of oil spills since the *Deepwater Horizon* disaster. *Crit. Rev. Anal. Chem.* **2023**, *53* (8), 1638−1697. Niles, S. F.; Chacón-Patiño, M. L.; Chen, H.; McKenna, A. M.; Blakney, G. T.; Rodgers, R. P.; Marshall, A. G. Molecular-level characterization of oil-soluble ketone/aldehyde photo-oxidation products by Fourier transform ion cyclotron resonance mass spectrometry reveals similarity between microcosm and field samples. *Environ. Sci. Technol.* **2019**, *53* (12), 6887−6894.

(6) Zito, P.; Podgorski, D. C.; Johnson, J.; Chen, H.; Rodgers, R. P.; Guillemette, F.; Kellerman, A. M.; Spencer, R. G.; Tarr, M. A.

Molecular-level composition and acute toxicity of photosolubilized petrogenic carbon. *Environ. Sci. Technol.* **2019**, *53* (14), 8235−8243.
(7) Ward, C. P.; Sharpless, C. M.; Valentine, D. L.; French-McCay, D. P.; Aeppli, C.; White, H. K.; Rodgers, R. P.; Gosselin, K. M.; Nelson, R. K.; Reddy, C. M. Partial photochemical oxidation was a dominant fate of Deepwater Horizon surface oil. *Environ. Sci. Technol.* **2018**, *52* (4), 1797−1805.
(8) Overton, E. B.; Adhikari, P. L.; Radović, J. R.; Passow, U. Fates of petroleum during the *Deepwater Horizon* oil spill: A chemistry perspective. *Front. Mar. Sci.* **2022**, *9*, 928576.
(9) Ward, C. P.; Armstrong, C. J.; Conmy, R. N.; French-McCay, D. P.; Reddy, C. M. Photochemical oxidation of oil reduced the effectiveness of aerial dispersants applied in response to the Deepwater Horizon spill. *Environ. Sci. Technol. Lett.* **2018**, *5* (5), 226−231.
(10) Farrington, J. W.; Overton, E. B.; Passow, U. Biogeochemical processes affecting the fate of discharged *Deepwater Horizon* gas and oil. *Oceanography* **2021**, *34* (1), 76−97.
(11) Hall, G. J.; Frysinger, G. S.; Aeppli, C.; Carmichael, C. A.; Gros, J.; Lemkau, K. L.; Nelson, R. K.; Reddy, C. M. Oxygenated weathering products of Deepwater Horizon oil come from surprising precursors. *Mar. Pollut. Bull.* **2013**, *75* (1−2), 140−149. S0025−326X(13)00441−4 [pii]
(12) McKenna, A. M.; Nelson, R. K.; Reddy, C. M.; Savory, J. J.; Kaiser, N. K.; Fitzsimmons, J. E.; Marshall, A. G.; Rodgers, R. P. Expansion of the analytical window for oil spill characterization by ultrahigh resolution mass spectrometry: Beyond gas chromatography. *Environ. Sci. Technol.* **2013**, *47* (13), 7530−7539.
(13) Chen, H.; Hou, A.; Corilo, Y. E.; Lin, Q.; Lu, J.; Mendelssohn, I. A.; Zhang, R.; Rodgers, R. P.; McKenna, A. M. 4 Years after the *Deepwater Horizon* Spill: Molecular Transformation of Macondo Well Oil in Louisiana Salt Marsh Sediments Revealed by FT-ICR Mass Spectrometry. *Environ. Sci. Technol.* **2016**, *50* (17), 9061−9069.
(14) Ruddy, B. M.; Huettel, M.; Kostka, J. E.; Lobodin, V. V.; Bythell, B. J.; McKenna, A. M.; Aeppli, C.; Reddy, C. M.; Nelson, R. K.; Marshall, A. G.; et al. Targeted petroleomics: Analytical investigation of Macondo well oil oxidation products from Pensacola Beach. *Energy Fuels* **2014**, *28* (6), 4043−4050.
(15) Harriman, B. H.; Zito, P.; Podgorski, D. C.; Tarr, M. A.; Suflita, J. M. Impact of Photooxidation and Biodegradation on the Fate of Oil Spilled During the *Deepwater Horizon* Incident: Advanced Stages of Weathering. *Environ. Sci. Technol.* **2017**, *51* (13), 7412−7421.
(16) Garrett, R. M.; Pickering, I. J.; Haith, C. E.; Prince, R. C. Photooxidation of crude oils. *Environ. Sci. Technol.* **1998**, *32* (23), 3719−3723. Dutta, T. K.; Harayama, S. Fate of crude oil by the combination of photooxidation and biodegradation. *Environ. Sci. Technol.* **2000**, *34* (8), 1500−1505. Ali, L.; Mantoura, R.; Rowland, S. The dissolution and photodegradation of Kuwaiti crude oil in seawater. Part 2: A laboratory photodegradation apparatus and photodegradation kinetics of a model seawater soluble hydrocarbon (phenanthrene). *Mar. Environ. Res.* **1995**, *40* (4), 319−335. Fernández-Varela, R.; Gómez-Carracedo, M.; Fresco-Rivera, P.; Andrade, J.; Muniategui, S.; Prada, D. Monitoring photooxidation of the Prestige's oil spill by attenuated total reflectance infrared spectroscopy. *Talanta* **2006**, *69* (2), 409−417.
(17) Vaughan, P. P.; Wilson, T.; Kamerman, R.; Hagy, M. E.; McKenna, A.; Chen, H.; Jeffrey, W. H. Photochemical changes in water accommodated fractions of MC252 and surrogate oil created during solar exposure as determined by FT-ICR MS. *Mar. Pollut. Bull.* **2016**, *104* (1−2), 262−268.
(18) Barron, M. G.; Carls, M. G.; Short, J. W.; Rice, S. D. Photoenhanced toxicity of aqueous phase and chemically dispersed weathered Alaska North Slope crude oil to Pacific herring eggs and larvae. *Environ. Toxicol. Chem.* **2003**, *22* (3), 650−660.
(19) Lee, R. F. Photo-oxidation and photo-toxicity of crude and refined oils. *Spill Sci. Technol. Bull.* **2003**, *8* (2), 157−162.
(20) Brohon, B.; Delolme, C.; Gourdon, R. Complementarity of bioassays and microbial activity measurements for the evaluation of hydrocarbon-contaminated soils quality. *Soil Biol. Biochem.* **2001**, *33* (7), 883−891. Morales-Caselles, C.; Kalman, J.; Riba, I.; DelValls, T. Comparing sediment quality in Spanish littoral areas affected by acute (Prestige, 2002) and chronic (Bay of Algeciras) oil spills. *Environ. Pollut.* **2007**, *146* (1), 233−240. Pelletier, E.; Delille, D.; Delille, B. Crude oil bioremediation in sub-Antarctic intertidal sediments: Chemistry and toxicity of oiled residues. *Mar. Environ. Res.* **2004**, *57* (4), 311−327.
(21) Roebuck, J. A., Jr.; Podgorksi, D. C.; Wagner, S.; Jaffé, R. Photodissolution of charcoal and fire-impacted soil as a potential source of dissolved black carbon in aquatic environments. *Org. Geochem.* **2017**, *112*, 16−21.
(22) Hazen, T. C. Lessons from the 2010 Deepwater Horizon accident in the Gulf of Mexico. *Hydrocarbons, Oils And Lipids: Diversity, Origin, Chemistry And Fate*; Springer International Publishing, 2020, 847−864. .
(23) Chen, H.; Laws, E. A.; Martin, J. L.; Berhane, T.-K.; Gulig, P. A.; Williams, H. N.; McFall-Ngai, M. J. Relative contributions of Halobacteriovorax and bacteriophage to bacterial cell death under various environmental conditions. *MBio* **2018**, *9* (4), 01202−01218.
(24) Dittmar, T.; Koch, B.; Hertkorn, N.; Kattner, G. A simple and efficient method for the solid-phase extraction of dissolved organic matter (SPE-DOM) from seawater. *Limnol. Oceanogr.: Methods* **2008**, *6* (6), 230−235.
(25) Kaiser, N. K.; Quinn, J. P.; Blakney, G. T.; Hendrickson, C. L.; Marshall, A. G. A Novel 9.4 Tesla FTICR Mass Spectrometer with Improved Sensitivity, Mass Resolution, and Mass Range. *J. Am. Soc. Mass Spectrom.* **2011**, *22*, 1343−1351.
(26) Rowland, S. M.; Robbins, W. K.; Corilo, Y. E.; Marshall, A. G.; Rodgers, R. P. Solid-phase extraction fractionation to extend the characterization of naphthenic acids in crude oil by electrospray ionization Fourier transform ion cyclotron resonance mass spectrometry. *Energy Fuels* **2014**, *28* (8), 5043−5048.
(27) Johnson, B. T. Microtox® toxicity test system—new developments and applications. *Microscale testing in aquatic toxicology*; CRC Press, 2018; pp. 201218.
(28) Campisi, T.; Abbondanzi, F.; Casado-Martinez, C.; DelValls, T.; Guerra, R.; Iacondini, A. Effect of sediment turbidity and color on light output measurement for Microtox® Basic Solid-Phase Test. *Chemosphere* **2005**, *60* (1), 9−15. Paul, J. H.; Hollander, D.; Coble, P.; Daly, K. L.; Murasko, S.; English, D.; Basso, J.; Delaney, J.; McDaniel, L.; Kovach, C. W. Toxicity and mutagenicity of gulf of Mexico waters during and after the deepwater horizon oil spill. *Environ. Sci. Technol.* **2013**, *47* (17), 9651−9659.
(29) Ward, C. P.; Overton, E. B. How the 2010 *Deepwater Horizon* spill reshaped our understanding of crude oil photochemical weathering at sea: A past, present, and future perspective. *Environ. Sci.: Processes Impacts* **2020**, *22* (5), 1125−1138.
(30) Aeppli, C.; Nelson, R. K.; Radovic, J. R.; Carmichael, C. A.; Valentine, D. L.; Reddy, C. M. Recalcitrance and degradation of petroleum biomarkers upon abiotic and biotic natural weathering of Deepwater Horizon oil. *Environ. Sci. Technol.* **2014**, *48* (12), 6726−6734.

https://doi.org/10.1021/acs.energyfuels.4c03951
Energy Fuels XXXX, XXX, XXX−XXX